World Conference on
Timber Engineering
Oslo 2023

DEFLECTION OF CANTILEVER CROSS-LAMINATED TIMBER DIAPHRAGMS UNDER IN-PLANE LOAD

Bibek Bhardwaj[1], Weichiang Pang[2], Michael Stoner[3], Douglas Rammer[4], Steve Pryor[5]

ABSTRACT: Diaphragms are used to transmit lateral loads to the vertical elements (e.g., shear walls) of the lateral force resisting system of a structure. The extent of deflection in diaphragms can determine what mechanism needs to be considered during design for transfer of forces to the vertical elements. Current design specifications do not provide equations that engineers can use to determine the deflections in cantilever Cross-Laminated Timber (CLT) diaphragms. In this paper, the CLT shear wall equation prescribed by 2021 Special Design Provisions for Wind and Seismic (SDPWS) was adapted to get an equivalent analytical equation for cantilever CLT diaphragm deflection. A full scale 6.1 m x 6.1 m (20 ft. × 20 ft.) cantilever CLT diaphragm was tested using displacement controlled cyclic protocol and the deformations at various regions of the diaphragms were measured. Analysis of test results suggests that the modified shear wall deflection equation for a cantilever CLT diaphragm based on SDPWS overpredicts the contribution due to bending and shear deformations.

KEYWORDS: CLT Diaphragm, Diaphragm Deflection, Cantilever, Deflection equation

1 INTRODUCTION

Deflection in diaphragms is an essential consideration for structural design. Excessive deflection in diaphragms is often undesirable as the stiffness of diaphragms can affect storey drifts [1]. The U.S. standard for Minimum Design Loads and Associated Criteria for Buildings and Other Structures (ASCE 7-22) [2] section 12.12.1 sets criteria for allowable design story drift limits. To quantify the distribution of shear forces to the vertical elements, diaphragms are often idealized to be completely flexible or rigid. Section 12.3.1.3 of ASCE 7-22 permits diaphragms to be idealized as flexible if the maximum in-plane diaphragm deflection is greater than twice the average deflection of adjoining elements of the vertical lateral force resisting system (VLFRS). For flexible diaphragms, shear forces are distributed to the VLFRS based on tributary area while for rigid diaphragms, shear forces are distributed based on the relative lateral stiffness of the elements of VLFRS. For light frame diaphragms, section 4.2.4 of the 2021 Special Design Provisions for Wind and Seismic (SDPWS) [3] provides three-term equations for determining in-plane deflections of cantilever diaphragms of cases of uniformly distributed load and concentrated load at the end of the diaphragm. Cross Laminated Timber (CLT) was introduced in the 2015 version of the National Design Specification for Wood Construction (NDS) [4] but such provisions are not yet available for cantilever CLT diaphragms. In this research, the equation for CLT shear walls provided by SDPWS was utilized to get an equivalent expression for deflections in a cantilever CLT diaphragm. The analytical equation was evaluated by comparing its predictions to the observations made during a full-scale test of a 6.1 m x 6.1 m (20 ft. × 20 ft.) cantilever CLT diaphragm.

2 BACKGROUND

In case of light frame diaphragms, the SDPWS provides a three and four-term equation for determining the end deflection of a simply supported diaphragm (equations C4.2.3-2 and C4.2.3-1 respectively) for uniformly distributed load case. For cantilever diaphragms, SDPWS provides three-term equations for determining in-plane deflections for both uniformly distributed and concentrated load at the end cases (equations 4.2-2 and 4.2-3 respectively).

The equation provided by SDPWS for deflection at the free end of a cantilever light frame diaphragm under concentrated point load (4.2-3) is as follows:

$$\delta_{dia} = \frac{8vL'^3}{EAW'} + \frac{vL'}{1000G_a} + \frac{\sum x'\Delta_c}{W'} \tag{1}$$

Where,

- δ_{dia} = deflection at free end of the diaphragm, in.
- v = unit induced shear, plf
- L' = length of diaphragm, ft.
- E = modulus of elasticity of diaphragm chords

[1] Bibek Bhardwaj, Clemson University, USA, bibekb@clemson.edu
[2] Weichiang Pang, Clemson University, USA, wpang@clemson.edu
[3] Michael Stoner, Clemson University, USA, mwstone@clemson.edu
[4] Douglas Rammer, Forest Products Laboratory, USA douglas.r.rammer@usda.gov
[5] Steve Pryor, Simpson Strong-Tie, USA spryor@strongtie.com

https://doi.org/10.52202/069179-0365

G_a	=	apparent diaphragm shear stiffness from nail slip and panel shear deformation, kip/in.
x'	=	distance from chord splice to free end of diaphragm
Δ_c	=	diaphragm chord splice slip, in.
W'	=	total width of the diaphragm, ft.

The principal modes of deflection for equation 1 are assumed to be deflection due to bending (of the chords, excluding slip), shear deformation (of the panels, excluding slip), shear deformation due to nail slip in the panels and deformation due to anchorage slip. In case of CLT diaphragms, one of the early attempts at quantifying deflections was carried out by Spickler et al. [5] in a horizontal CLT diaphragm deflection design example. The equation presented in the design example was expanded from the four-term diaphragm deflection equation for light frame diaphragms. Unlike light frame diaphragms, where the flexural and shear members are distinct (the flexural deformation is considered only for the chord members while shear deformation is considered only for the sheathing material), for CLT diaphragms, the CLT panels themselves were designed as chord and shear members, capable of withstanding both bending and shear.

In the 2021 version of the SDPWS, section 4.5.2 suggests determining the deflection in a CLT diaphragm using principles of engineering mechanics without explicitly providing an equation. To help engineers and design practitioners come up with an estimate for diaphragm deflection for different layouts and configurations, Lawson et al. [6] have provided recommendations to estimating the various components of deflections in a CLT diaphragm.

Section 4.6.2 of SDPWS suggests determining deflection in CLT shear walls using principles of engineering mechanics as well but provides an equation for calculating the deflection in appendix B.4. Commentary on appendix B.4 provides further insights to the equation and its assumptions. Due to the similarity in layout between a CLT shear wall and a cantilever CLT diaphragm, an equivalent expression for CLT diaphragms can be determined based on the equations for CLT shear walls in the SDPWS.

The equivalent expression for free end deflection in a CLT diaphragm under concentrated point load at the end, generalized for different fastener types (not just nailed spline connection) is given as follows:

$$\delta_{dia} = \frac{576 v P_w L^3}{EI_{eff(in-plane)}} + \frac{vL}{GA_{eff(in-plane)}} + n_0 e_0 + e_{90}\frac{L}{P_W} + \frac{\Delta_a}{W}L \quad (2)$$

Where,

δ_{dia}	=	deflection at free end of the diaphragm, in.
v	=	unit induced shear, plf
P_W	=	individual panel width, ft.
L	=	length of diaphragm, ft.
$EI_{eff\ (in\text{-}plane)}$	=	effective in-plane bending stiffness of CLT panel, lbs-in^2
$GA_{eff\ (in\text{-}plane)}$	=	effective in-plane shear stiffness of the CLT panel, lbs/in. of panel length
n_0	=	number of locations for longitudinal (parallel to load) shear fasteners
e_0	=	deflection at each fastener location in., (= 0 for single panel diaphragm)
e_{90}	=	transverse fastener slip, in.
Δ_a	=	slip at the anchorage, in.
W	=	total width of the diaphragm, ft.

It should be noted that equation 2 uses customary units used in the US and includes an implicit unit conversion factor in the first term for calculating the deformation due to in-plane panel bending. Modification of equation 2 for SI units would require a modification to that factor.

Figure 1 shows all the deformation modes considered for the equation 2.

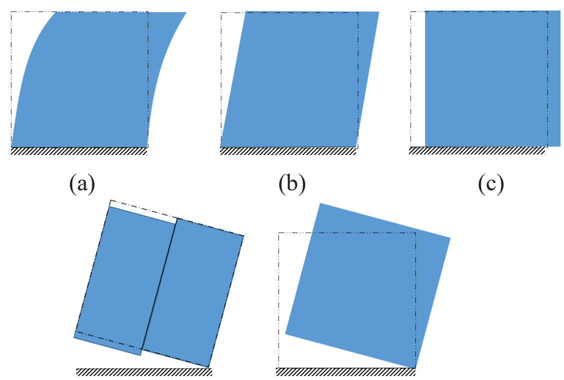

Figure 1: *Deformation modes considered (a) Bending, (b) Shear, (c) Longitudinal shear fastener slip (d) Transverse shear fastener slip, and (e) Anchorage slip.*

This paper takes results from an experimental test conducted on a cantilever CLT diaphragm and compares the deflections observed to the predictions made by the SDPWS based equation (equation 2).

3 EXPERIMENTAL SETUP

3.1 LAYOUT

A 6.1 m × 6.1 m (20 ft. × 20 ft.) CLT diaphragm was tested destructively using displacement-controlled loading based on CUREE (Consortium of Universities for Research in Earthquake Engineering) [7] cyclic protocol [8]. The diaphragm was composed of four 1.5 m × 6.1 m (5 ft. × 20 ft.) panels resting on three 6.1 m (20 ft.) long 17.1 cm (6.75 in.) wide and 34.9 cm (13.75 in.) deep glulam beams along the short edges of the panels as shown in Figure 2. The long edges of the panels were connected using a 2.5 cm (1 in.) thick plywood surface spline using 16d common nails at 7.6 cm (3 in.) c/c as shown in Figure 2. The detailing for the surface spline

https://doi.org/10.52202/069179-0365

connection is shown in Figure 3. The CLT panels were connected to the glulam beams underneath using Simpson strong Tie's SDWS22800DB screws at 15.2 cm (6 in.) c/c on the two outside glulam beams and 20.3 cm (8 in.) c/c on the middle glulam beam (Figure 2). Custom made Simpson Strong Tie hold-downs were installed 25.4 cm (10 in.) from the edges on both sides (Figure 2).

The load was applied using a hydraulic actuator attached to the free end glulam beam.

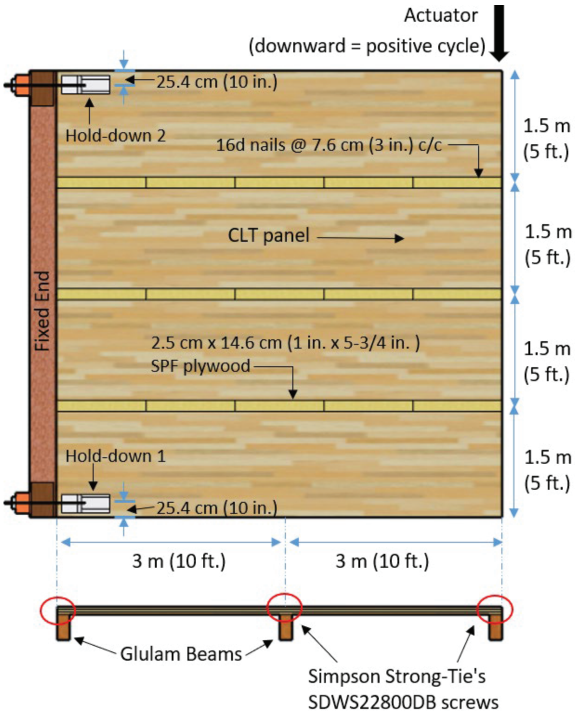

Figure 2: *Layout for the diaphragm test*

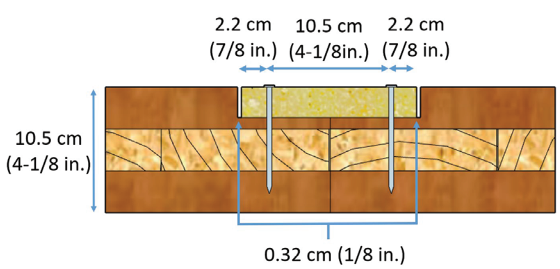

Figure 3: *Surface spline detail*

3.2 DESIGN OF CLT DIAPHRAGM

The diaphragm was designed (for seismic considerations) using recommendations from a design example [5] and SDPWS 2021. The diaphragm had a Load and Resistance Factor Design (LRFD) in-plane shear capacity of 98.3 kN (22.1 kip) based on the strength of the surface spline nailed connection. The Allowable Stress Design (ASD) capacity of the diaphragm was 70.2 kN (15.8 kip). The CLT-glulam screws were designed to have an additional 61% capacity over the design forces expected at the CLT glulam interface. All other components of the diaphragm were design to have at least two times the capacity compared to the design level forces at the respective component per the requirements of SDPWS 2021. The LRFD capacity summary for the diaphragm components is given in Table 1 [8].

Table 1: *LRFD capacities of Diaphragm Components (seismic design)*

Component	Required Capacity* kN (kip)	Design Capacity kN (kip)	Strength Ratio**
Panel-Panel nailed surface spline	98.3 (22.1)	98.3 (22.1)	1:1
Panel-Glulam screws	98.3 (22.1)	158.4 (35.6)	1.6:1
Tension Chord	222.4 (50)	323.8 (72.8)	2.9:1
Compression Chord	222.4 (50)	327.4 (73.6)	2.9:1
Hold-downs	222.4 (50)	560.5 (126)	5:1

*required capacity for non-shear elements is twice the capacity obtained using design shear forces

**ratio of design capacity to capacity obtained using design shear forces

3.3 INSTRUMENTATION SETUP

Figure 4 and Figure 5 show the location of the various string potentiometers used in the diaphragm test to track component deformations [8]. The load deformation response on the free end glulam beam was captured by the sensors in the hydraulic actuator. Figure 4 also shows the two load cells (LC1 and LC2) used to capture the uplift force experienced by the diaphragm at the hold-down location.

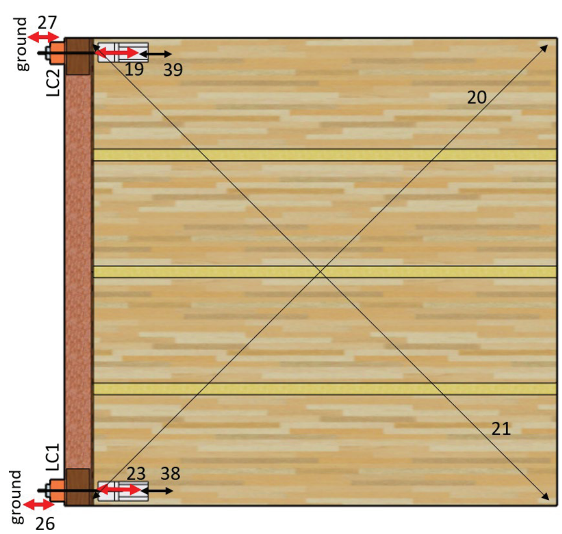

Figure 4: *String pot and hold-down layout on the top of the diaphragm*

https://doi.org/10.52202/069179-0365

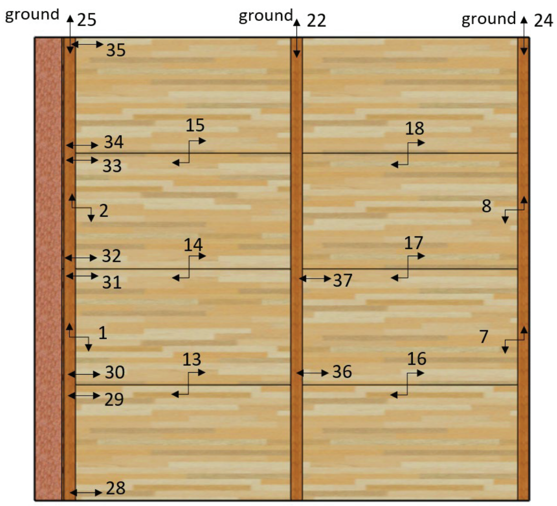

Figure 5: *String pot layout on the bottom of the diaphragm*

It should be noted that the instrumentation was not setup to capture the bending and shear deformations (described in Figure 1a and Figure 1b).

4 RESULTS AND OBSERVATIONS

4.1 OVERALL BEHAVIOUR OF DIAPHRAGM SETUP

Figure 6 shows the hysteresis for the applied displacement vs force observed for the diaphragm test setup [8]. The summary of the test results is shown in Table 1 [8]. The diaphragm setup displayed a relatively symmetrical behaviour for positive and negative cycles. The average initial stiffness of the setup was 24.1 kN/cm (13.8 kip/in.). The peak capacity of the diaphragm exceeded its LRFD capacity by a factor of 1.7. Through the observation of deformations during the test, it was inferred that the peak capacity of the diaphragm was primarily governed by the capacity of its surface spline nailed connection which was consistent with the design detail. Deformations could be visually observed on the surface spline nailed connection, the CLT-glulam screw connection and in the hold-down connection. No significant bending and shear deformation of the panels could be visually observed during the test. Thus, the primary energy dissipation mechanism was concluded to be governed by the various mechanical fasteners utilized in the diaphragm setup, with the CLT panels acting as rigid members. The mechanical fasteners also induced ductility to the diaphragm.

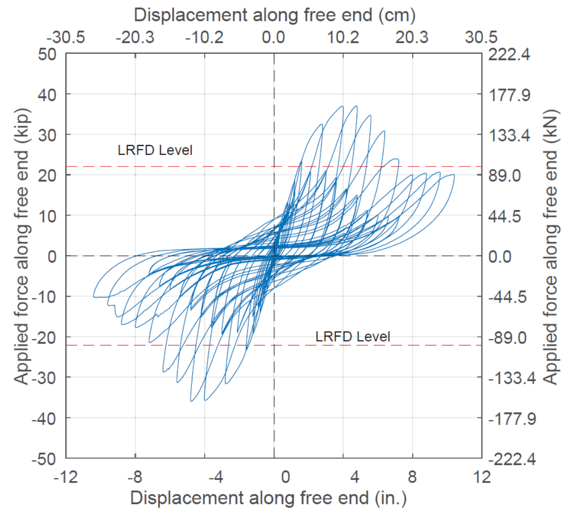

Figure 6: *Force vs displacement hysteresis for the diaphragm test*

Table 2: *Summary of the Diaphragm test*

Design LRFD load	98.3 kN (22.1 kip)
Peak positive load	164.5 kN (37 kip)
Peak positive displacement	11.4 cm (4.47 in.)
Initial stiffness (positive)	22.4 kN/cm (12.8 kip/in.)
Peak negative load	160 kN (36 kip.)
Peak negative displacement	11.2 cm (4.41 in.)
Initial stiffness (negative)	25.6 kN/cm (14.6 kip/in.)
Average peak/LRFD strength	1.7

4.2 DEFLECTIONS AT VARIOUS FORCE LEVELS

Figure 7 and Figure 8 show the contribution of fastener deformation to total diaphragm deflection at various force levels for positive and negative cycles respectively. The force level values in the figures indicate the first time those values were reached during the diaphragm test. The diaphragm level deformations were calculated from the fastener level deformations for nailed surface spline slip (transverse shear fastener), screw slip (longitudinal shear fastener) and slip in the hold-down assembly (anchorage) using the equation 2. The bending and shear deformations which were back calculated by subtracting all other deformations from observed diaphragm deflection. This was done because the test setup did not have sufficient instrumentation to properly isolate contribution due to bending and shear deformations.

Figure 7 and Figure 8 also show the SDPWS based (theoretical) estimates for total bending and shear deformations while Table 3 shows the numerical values.

Table 3: *SDPWS based estimates for bending and shear deformations at various force levels.*

Force level kN (kip)	Bending Def. cm (in.)	Shear Def. cm (in.)
22.2 (5)	0.208 (0.082)	0.107 (0.042)
44.5 (10)	0.417 (0.164)	0.213 (0.084)
70.3 (15.8) - ASD	0.658 (0.259)	0.337 (0.133)
98.3 (22.1) - LRFD	0.921 (0.362)	0.472 (0.186)

https://doi.org/10.52202/069179-0365

The plots suggest that SDPWS based calculation overpredicts the contributions due to bending and shear deformations in a cantilever CLT diaphragm.

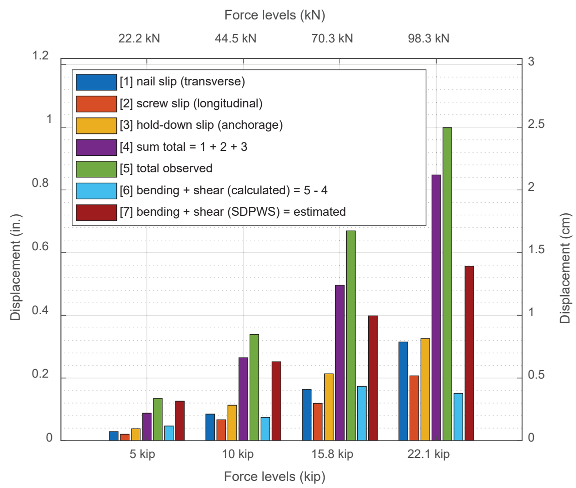

Figure 7: *Contribution of fastener deformation to total diaphragm deformation for positive cycle, ASD = 70.3 kN (15.8 kip), LRFD = 98.3 kN (22.1 kip)*

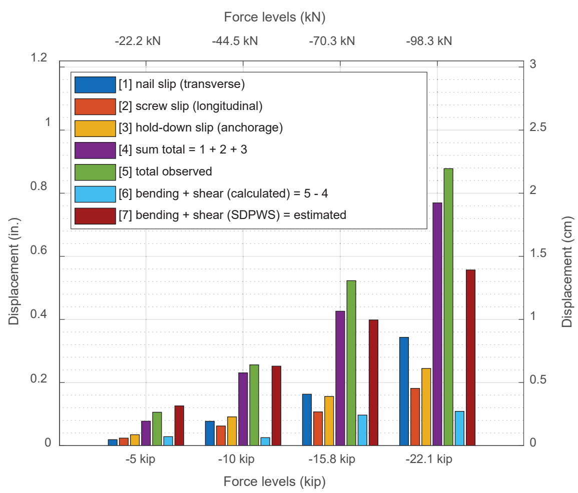

Figure 8: *Contribution of fastener deformation to total diaphragm deformation for negative cycle, ASD = 70.3 kN (15.8 kip), LRFD = 98.3 kN (22.1 kip)*

The back calculated values for bending and shear deformations were 34.8% and 26.8% of the total diaphragm deflections at force level of 22.2 kN (5 kip) for positive and negative cycles respectively. At LRFD level of 98.3 kN (22.1 kip), the back calculated values for bending and shear deformations were 15.1% and 12.4% of the total diaphragm deflection for positive and negative cycles respectively. The bending and shear deformation predicted by SDPWS would have been 93.6% and 119% (i.e., exceed observed diaphragm deflection value) at 22.2 kN (5 kip) for positive and negative cycles respectively. Similarly, bending and shear deformations predicted by SDPWS would have been 55.8% and 63.4% of the total predicted deflection at LRFD level for positive and negative cycles respectively.

The deformations also suggest that the bending and shear deformations were more significant at smaller load levels. It is speculated that as the load levels increased, the bending and shear deformation increased linearly while the other deformations increased non-linearly (at a higher rate), thus leading to lower contribution of bending and shear deformation at higher load levels as the fasteners which have started to deform and yield begin to experience more deflection relative to the CLT panels in bending and shear.

5 CONCLUSIONS

During design, the ratio of deflection in diaphragm to the adjoining components of the VLFRS can be utilized to idealize flexible, rigid or semi rigid diaphragm behaviour which governs the mechanism for force transfer to the vertical elements. The various mechanisms contributing to deflections in cantilever CLT diaphragms were investigated. Observation of deflection data from the test suggested that the equation derived using the in SDPWS equation for CLT shear wall over predicts the contribution of bending and shear deformations. Further experimental testing with instrumentation setup for capturing bending and shear deformations seems necessary to develop equations capable of providing a more accurate prediction for those terms.

ACKNOWLEDGEMENT

The material present in this paper is based on work supported in part by the US Department of Agriculture (USDA) Forest Services and the US Endowment for Forestry and Communities Grant No. E17-96. Any opinions, findings, conclusions, and recommendations presented in this paper are those of the authors and do not necessarily reflect the views of the USDA and the US Endowment for Forestry and Communities. The authors would also like to thank Lancelot Reres, Sovanroth Ou, Harsh Bothra and Jayson Leonard for their help and assistance throughout the project.

REFERENCES

[1] D'Arenzo, G., Casagrande, D., Reynolds, T., & Fossetti, M. (2019). In-plane elastic flexibility of cross laminated timber floor diaphragms. Construction and Building Materials, 209, 709-724. doi: 10.1016/j.conbuildmat.2019.03.060.

[2] Structural Engineering Institute: Minimum design loads for buildings and other structures. ASCE 7, Reston, VA. 2022

[3] American Wood Council: Special Design Provisions for Wind and Seismic, 2021.

[4] American Wood Council: National Design Specification for Wood construction. 2018

[5] Spickler, K., Closen, M., Line, P., and Pohll, M. (2015),. Cross Laminated Timber Horizontal Diaphragm Design Example. Structurlam-CrossLam.

[6] Lawson, J., Breneman, S., & Lo Ricco, M. (2023): Wood Diaphragm Deflections. Part I: Generalizing Standard Equations Using Mechanics-Based

Derivations for Panel Construction. ASCE Journal of Architectural Engineering
[7] Krawinkler, H., Parisi, F., Ibarra, L., Ayoub, A., & Medina, R. (2001): Development of a Testing Protocol for Woodframe Structures. Department of Civil and Environmental Engineering, Stanford University.
[8] Bhardwaj, B., Pang, W., & Stoner, M. (under review). Experimental Characterization of Cantilever Cross-Laminated Timber Diaphragms under In-plane Shear Load. Journal of Structural Engineering.

https://doi.org/10.52202/069179-0365